



Bone Conduction Transducers:  
output force dependency on load condition

Diana Cortés

Department of Signals and Systems  
Chalmers University of Technology  
SE-412 96 Göteborg, Sweden

September 4, 2002

## Abstract

The aim of this investigation is to determine the output force variability of the new bone conduction transducer, called balanced electromagnetic separation transducer (BEST), and of the conventional transducer from Radioear B71. The variability of the output force is dependent on different load conditions. The loads used were the mechanical impedance of the skull of thirty test persons and the mechanical impedance of the artificial mastoid (AM) 4930 from Brüel & Kjær. The hypothesis is that BEST has less variability since it has inherent damping of the spring elements, while B71's damping takes place through the skin and the soft tissue, i.e. the damping is mostly patient dependent. The output force of the transducers were determined in three different ways:

1. Transducer modelled as a four pole equivalent.
2. Transducer modelled as an impedance analogy lumped parameter model.
3. Direct measurement using the AM (not completed in this study).

Models of the transducers were determined from frequency response measurements simply called variables in this report.

As it was expected the variation of the output force calculated with the mechanical impedance of the test persons was less for BEST than for B71. For BEST, the standard deviation of the force is approximately +2 to -3 dB at 316 Hz while for B71 the deviation at 200 to 500 Hz is up to +4 to -10 dB. Both transducers show greater load dependency at higher frequencies. BEST has a standard deviation range from +0.8/ - 1 dB to +3/ - 5 dB in the frequency region from 0.8 to 3 kHz. B71 shows a standard deviation in force of +4 to -6 dB from 1.2 to 10 kHz.

The results also show that, though the mechanical impedances of the test objects and the impedance of the artificial mastoid are very different (about 7 dB relative to 1 Ns/m between the mean and AM) the output force does not differ as much as the impedances. Comparing the output forces with BEST and the two impedances (mean human skull and AM), it yields lower force magnitude when the force is calculated with the mean value of the impedance of the test objects (up to 10 dB rel 1 N/V for the frequencies from 1.3 to 10 kHz). B71 shows also lower force magnitude with the impedance of the test persons than with the impedance of AM but beginning at a lower frequency than BEST, (from 6 up to 10 dB rel 1 N/V for 0.4 to 10 kHz).

Further, BEST shows approximately 5 dB higher output force in the low frequency range of 100 to 400 Hz than B71, with both types of mechanical impedance, which is an important advantage for BEST due to the distortion found by Håkansson (2002) at lower frequencies for B71. When the output force is calculated with the mean value of the impedances of the subjects, B71 gives higher amplitude than BEST, about 10 dB rel 1 N/V, in the frequency region from 1.3 to 10 kHz, while for the force determined with the impedance of the AM the higher force level starts at 400 Hz becoming equal to that of BEST at 1 kHz to increase again the remaining frequency range.

Since the resonances of the variables  $Z_{21}$  and  $Z_{12}$  did not occur at the same frequency it leads to some artifacts that should be disregarded. It is of interest to calculate the value of the components of the transducers and make new calculations of the output force to be sure that the artifacts vanish.

## Contents

<b>1</b>	<b>Introduction</b>	<b>1</b>
<b>2</b>	<b>Material, Methods and Apparatus</b>	<b>2</b>
2.1	Mechanical Impedance Measurement . . . . .	2
2.2	Two-port network - frequency response measurements . . . . .	5
2.3	The stimulation force . . . . .	10
<b>3</b>	<b>Results</b>	<b>12</b>
3.1	Mechanical impedance . . . . .	12
3.2	Two-port frequency response functions . . . . .	12
3.3	The stimulation force . . . . .	12
<b>4</b>	<b>Discussion</b>	<b>24</b>
<b>5</b>	<b>Conclusions</b>	<b>27</b>
<b>6</b>	<b>Acknowledgment</b>	<b>28</b>

## List of Figures

1	Air view of measurement setup . . . . .	3
2	Measurement setup . . . . .	4
3	Four pole equivalent . . . . .	6
4	Model of the bone conduction transducer . . . . .	6
5	Measurement of the variable $Z_{11}$ . . . . .	7
6	Measurement of the variable $Z_{21}$ . . . . .	8
7	Measurement of the variable $Z_{12}$ . . . . .	9
8	Measurement of the variable $Z_{22}$ . . . . .	10
9	Magnitude and phase of mechanical impedance of test objects and AM . . . . .	13
10	Mechanical impedance of the skull with different static forces .	14
11	Magnitude and phase of $Z_{11}$ with BEST and B71 . . . . .	15
12	Magnitude and phase of $Z_{21}$ with BEST and B71 . . . . .	16
13	Magnitude and phase of $Z_{12}$ with BEST and B71 . . . . .	17
14	Magnitude and phase of $Z_{22}$ with BEST and B71 . . . . .	18
15	The stimulation force (SF) of BEST and B71 . . . . .	19
16	Mean value and standard deviation of stimulation force for both transducers . . . . .	20
17	SF for BEST and B71 with two different impedances . . . . .	22
18	Comparison of SF with mean value impedance and with AM impedance . . . . .	23

## 1 Introduction

Conventional bone conduction transducers of the variable reluctance type used in clinical audiometric testing of patients with different hearing impairments are usually calibrated with commercially available artificial mastoids that should have identical mechanical impedance as a normal patient in order to avoid pronounced interference between the transducer and the impedance of the patient. Therefore, if the impedances are not identical, the test result might not be as accurate as desired for the design purpose of an adequate hearing aid aimed to help the patient in question. Some bone conduction transducers have not internal damping making their characteristics, for instance the output force, strongly patient dependent since the damping is performed by the skin and underlying tissue of the patient.

The new bone conduction transducer called the balanced electromagnetic separation transducer, BEST, has inherent damping on the internal spring suspension which hypothetically should make it less patient dependent resulting in smaller variations in output force and contributing to more accurate testing results. Håkansson (2002) investigated the main characteristics, i.e. frequency response function, distortion and electrical input impedance, of two bone conduction transducers, BEST and B71 from Radioear, and found that BEST had higher amplification, lower distortion and higher electrical input impedance than B71. Thus, BEST constitutes a significant improvement of the functional quality of a bone conduction transducer which is due to the design with the balanced armature and the separated static- and signal fluxes. It is of interest to determine how the output force of the transducers are affected by the load condition. For that reason a new study has to be made considering the differences in mechanical impedance that human beings can present and the model variables of the transducers, that may be measured or calculated.

The aims of this investigation are then to:

- measure the mechanical point impedance (skin impedance) of a larger number of living subjects.
- model the transducers as a four pole equivalent and measure corresponding frequency response functions (FRF) and,
- with the impedances and the model variables determine the variability of the output force of the transducer assuming that the input voltage is constant.

The mechanical impedance of the artificial mastoid 4930 from B&K is also used as a load  $Z_L$  for comparison reasons.

## 2 Material, Methods and Apparatus

A group of thirty normal hearing subjects participated in the measurement of mechanical point impedance of the temporal bone without skin penetration (Skin impedance). The group, mostly colleagues at the department of Signal and Systems, consisted of 18 males and 12 females with ages between 22 and 51 with a mean of 30.6 years.

The measurements were performed with a two channel FFT-analyzer HP-3562A from Hewlett Packard, a mini-shaker type 4810 from Brüel & Kjær (B&K), the impedance heads 8000 and 8001 from B&K, the charge amplifiers type 2635 and 2651 from B&K and a power amplifier, Sony TA-N220. The mechanical impedance of the artificial mastoid B&K 4930 was also measured for reference purpose. The bone conduction transducer was modelled as a four pole equivalent or a two-port network. A two-port network has four frequency response functions or variables that have been measured. The transducers used in the measurement of the model parameters were: B71 nr. 86-5 from Radioear and the balanced electromagnetic separation transducer BEST nr. 3. The latter is called B3 in this report. Both transducers were encased in the same type of plastic housing. The weight varies, however. The B71 has a weight of 19.2 grams and BEST has a weight of 13 grams.

### 2.1 Mechanical Impedance Measurement

Mechanical impedance,  $Z$ , is a complex quantity that can be defined as the resistance of a structure to be set in motion. A dynamic force,  $F(j\omega)$ , applied to the structure will result in a certain velocity of the structure,  $v(j\omega)$ , in accordance with equation (1) where  $\omega$  is the excitation angular frequency. Both the magnitude and the phase of the applied force and the resultant velocity have to be determined for an accurate and complete measurement. Moreover, measurements have to be made at a large number of frequencies to obtain an acceptable frequency resolution.

$$Z(j\omega) = F(j\omega)/v(j\omega) \quad (1)$$

The impedance head type 8000 and the necessary adaptors were pressed against the right side of the head with a static force  $\mathbf{F}$ , (approx. 5.9 N) generated by a weight (599 grams) as shown in figure 1. The neck was resting on a V-formed cushion used to stabilize and reduce the movement artifacts from the head, avoiding contribution to the skin impedance. The impedance head was always placed on the flattest part of the mastoid portion of the temporal bone in order to obtain maximum contact with the skin.

The mini-shaker 4810 was supplied with the source signal of the FFT analyzer HP-3562A via a signal amplifier. Charge amplifiers amplified the signals from the B&K impedance head type 8000. The signal for the output force  $F$  in equation (1) was registered on channel two and the acceleration signal on channel one. A complete diagram of the measurement setup is shown in figure 2. Both random noise signal and a sinus sweep signal were used in all measurements in this study.

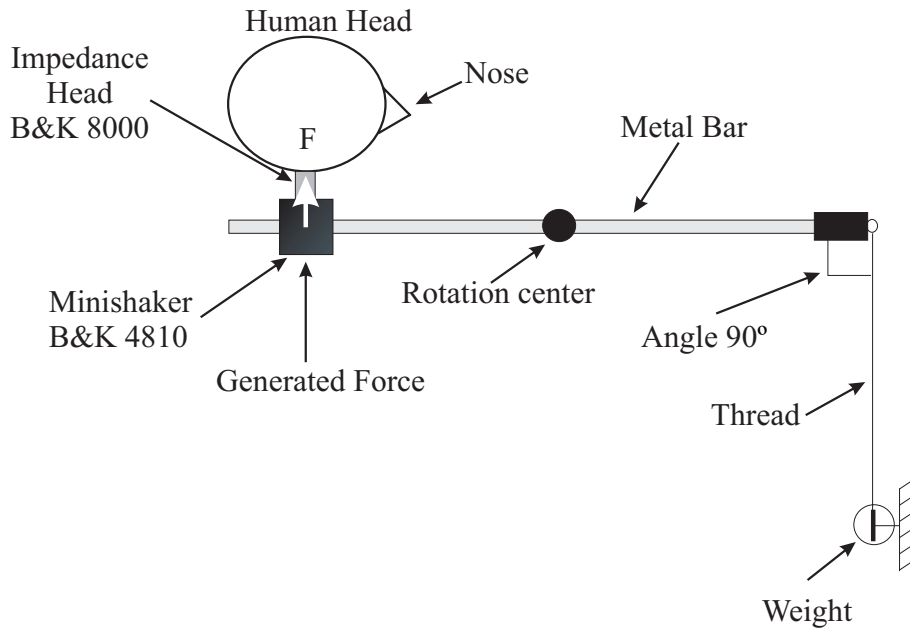


Figure 1: Mechanical impedance measurement setup seen from the air. The direction of the pressing static force  $\mathbf{F}$  is shown with a white arrow.

Before starting the measurements, a calibration process for the impedance head B&K 8000 was made. This calibration consisted of measurement of the apparent mass (force/acceleration) of a known mass ( $m = 49.9$  grams). The sensitivity of the analyzer was then adjusted so that its output at 0.1 kHz agreed with the known mass plus the mass,  $m_0 = 1.1$  grams, above the force gauge of the impedance head. The adjustment was made in the engineer units (EU) on channel two of the FFT-analyzer, with a value of 98 EU/V. A new measurement was made without loading the impedance head in order to get the apparent mass of the mass above the force gauge inside the impedance head for future compensation in the calculation of the mechanical impedance.

The skin impedance was also measured with four different weights, (300, 400, 500 and 600 grams) corresponding to 3, 4, 5 and 6 Newton, to observe how the impedance of the skull changes with different static forces.

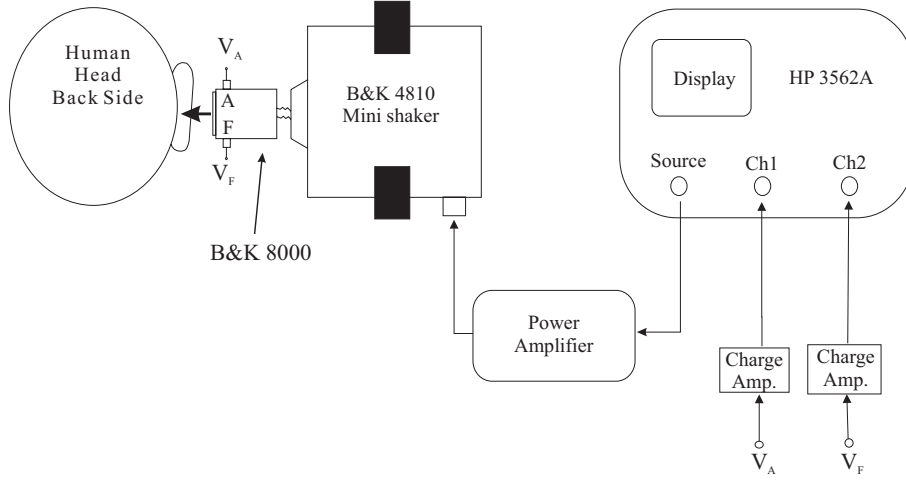


Figure 2: Setup for the measurement of mechanical impedance.

A “quality” factor of the estimated frequency response is the coherence function  $\gamma^2(jf)$ , where  $0 < \gamma^2(jf) < 1$ . Under ideal circumstances, the coherence function  $\gamma^2(jf)$  is unity. The coherence function  $\gamma^2(jf)$  was examined for each person, to consider if the measurement should be accepted or not. The acceptance limit was  $\gamma^2(jf) > 0.95$ . In order to achieve maximum signal-to-noise ratio, the measurements were performed at a loudness level as high as possible but still comfortable for the test person.

Applying the signal via a power amplifier, vibrations were generated to the mini-shaker B&K 4810. The impedance head was rigidly attached to the mini-shaker. Force and acceleration outputs from the impedance head were amplified by charge preamplifiers B&K 2651 and B&K 2635, respectively. From the measured frequency response  $F/A$ , the apparent mass of the mass above the force gauge was subtracted and the acceleration was integrated in order to convert it into velocity. This can easily be done with the FFT analyzer by multiplying  $F/A$  by  $j\omega$ , where  $\omega = 2\pi f$  and  $j$  is the complex constant. The same calculation can also be accomplished in Matlab, which was the case in this study.

The FFT analyzer computes the mechanical point impedance  $Z(jf)$  with the two channels cross spectrum  $S_{FA}$  and the channel one power spectrum  $S_{AA}$  according to equation (2), where the subscript A stands for acceleration and the subscript F stands for force. The minus sign compensates for the sign shift introduced by the accelerometer.

$$Z(jf) = -j\omega \cdot \frac{S_{FA}}{S_{AA}} \quad (2)$$

With random noise, averaging is necessary to achieve an acceptable signal-to noise ratio. Thirty consecutive time records ( $n = 30$ ) have been used for the averaging process, since they are enough to reduce the stationary random noise, but not too many to make the total measurement too long and annoying for the test person. The total measurement time was approximately 45 seconds for the random noise and approximately 90 seconds for the sinus sweep. No averaging was used when the sinus sweep measurements were made.

The overall accuracy of the mechanical point impedance measurement with the present method and apparatus is dependent on several factors of which the following probably cause the most serious errors: (1) poor signal-to-noise ratios and nonlinearities, i.e., low coherence values; (2) calibration accuracy of gain factors; (3) interaction of the measuring force gauge compliance with the measured impedance and imperfect mass compensation; and (4) bias errors due to noise in the acceleration channel. The magnitude accuracy of the present measurement apparatus was estimated to +20% to -10% for 100 to 400 Hz and  $\pm 10\%$  for 400 Hz to 10 kHz, the phase error was estimated to  $\pm 9^\circ$  for 100 Hz to 5 kHz and  $\pm 15^\circ$  for 5 to 10 kHz. These numbers are based on a random error corresponding to a coherence value of 0.95 and a confidence interval of 95%, a channel-to-channel match error and calibration error of  $\pm 3.5\%$  in magnitude and  $\pm 5^\circ$  in phase. Further details of error analysis can be found in Bendat and Piersol (1980).

## 2.2 Two-port network - frequency response measurements

The second step in this study was to model the bone conduction transducer as a two-port network. Figure 3 shows the model with the variables.  $V_1$  indicates the voltage over the input of the transducer,  $i_1$  the current into the transducer,  $V_2$  is the output voltage corresponding to the output force of the transducer and  $i_2$  is the current corresponding to the velocity into the transducer, according to the mechanical circuit analogy.  $Z_L$  is the load impedance.

Figure 4 shows the circuit elements in the transducer model.  $R_{Cu}$  represents the copper losses of the wires in the electrical part,  $\omega R$  stands for the magnetic and eddy current losses,  $L$  is the inductance of the coil and the voltage source  $g \cdot v$  can actually be represented with an equivalent impedance or motional impedance  $Z_{eq} = g \cdot v / i_1$ , where  $g$  is the transformation constant.

In the mechanical part of the transducer, the velocity is indicated by  $v$  and the transformation factor is the voltage source  $g \cdot i_1$ ; the input impedance

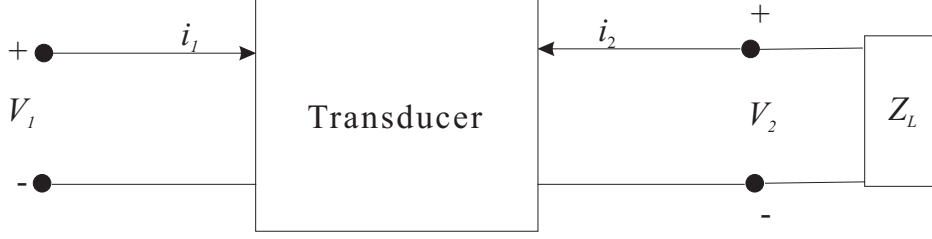


Figure 3: Bone conduction transducer model as a two-port network with the load  $Z_L$ .

of the mechanical part of the transducer is denoted with  $Z_M = g \cdot i_1/v$ . The motional impedance can now be written  $Z_{eq} = g^2/Z_M$ .  $C_1$  is the compliance of the suspension maintaining the air-gap of the transducer. The damping of the suspension springs is denoted  $r_1$ . The massive part of the transducer has a mass  $m_1$ , and the mass of the bobbin, coil, poles, plate and one third of the housing is represented with  $m_2$ . The housing compliance and damping are  $C_2$  and  $r_2$ , respectively. Two thirds of the housing has the mass  $m_3$ . The masses are different for both transducers. Finally,  $Z_L$  is the load, which in this study is constituted of the mechanical impedances of the skull and the AM.

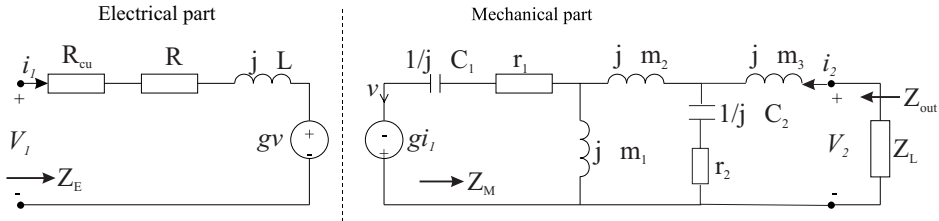


Figure 4: Model of the bone conduction transducer

The objective of this model was to obtain the transfer function: output force of the transducer over input voltage into the transducer, through measurable variables, the mechanical impedance of the 30 objects and the mechanical impedance of the artificial mastoid as well. The model can be written as in equation (3) below.

For this part of the work, the impedance head type 8001 was used due to the attachment facility to another apparatus, which would not be possible with the B&K type 8000 used in the mechanical impedance measurement.

$$\begin{pmatrix} V_1 \\ V_2 \end{pmatrix} = \begin{pmatrix} Z_{11} & Z_{12} \\ Z_{21} & Z_{22} \end{pmatrix} \begin{pmatrix} i_1 \\ i_2 \end{pmatrix} \quad (3)$$

From equation (3) the different variables  $Z_{11}$ ,  $Z_{21}$ ,  $Z_{12}$  and  $Z_{22}$  can be expressed in a manner that makes it possible to measure them assuming certain conditions. The calibration procedure was the same as described in section 2.1. However, there was a difference in weight. A little cone, with a weight of 2.15 grams, was used to attach the transducer to the B&K 8001 and the mass above the force gauge in the B&K 8001 is 2.2 grams. Thus, when compensating the mechanical output impedance  $Z_{22}$ , the apparent mass of the cone and the mass above the force gauge,  $m_{k0}$ , had to be subtracted from the measured frequency response  $F/A$ . Each FRF-measurement was performed using the transducers B71 and the BEST in the place of the transducer appearing in the figures below.

The first variable  $Z_{11}$  can be written as in equation (4) if assuming that the velocity  $i_2$  is zero. This can be performed by adapting the transducer to a mass much heavier than the mass of the transducer. The frequency response measured with the HP-3562A is  $V_1/V_S$ , where  $V_S$  is the amplified source voltage.

$$Z_{11} = \frac{V_1}{i_1} = \frac{V_1}{(V_S - V_1)/R} = \frac{V_1}{V_S} \frac{R}{(1 - \frac{V_1}{V_S})} = Z_E \quad (4)$$

In figure 5 the measurement setup for  $Z_{11}$  is illustrated, here  $R$  is a resistor of  $10 \Omega$ . A power amplifier Sony TA-N220 amplifies the source signal. Notice that the variable  $Z_{11}$  is the same as the electrical input impedance,  $Z_E$ , of the transducer when it is unloaded ( $Z_L = \infty$ ).

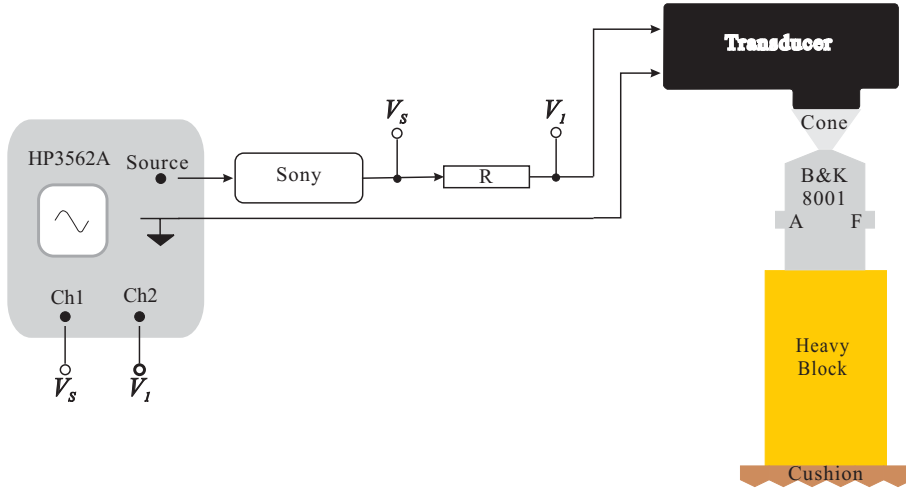


Figure 5: Measurement of the variable  $Z_{11}$ .

The second variable  $Z_{21}$  can also be measured assuming no output velocity, i.e.  $Z_L = \infty$ , as for the first variable  $Z_{11}$ . To measure variable  $Z_{21}$ , the

already measured variable  $Z_{11}$  was used as indicated in equation (5). The measured voltage  $V_2$  has to be compensated in order to achieve the output force signal  $F$  from the impedance head.

$$Z_{21} = \frac{F}{i_1} = \frac{F}{V_1/Z_{11}} = \frac{V_2}{\alpha_F} \cdot \frac{Z_{11}}{V_1} = \frac{V_2}{V_1} \cdot \frac{Z_{11}}{\alpha_F} \quad (5)$$

The compensation factor  $\alpha_F = 0.391$  V/N was calculated according to the sensitivity of the impedance head given in the head calibration chart and the sensitivity of the B&K charge amplifier type 2651, respectively as shown in equation (6). Figure 6 illustrates the measurement setup of  $Z_{21}$ . The measured frequency response was  $V_2/V_1$ .

$$\alpha_F = 391 \frac{pC}{N} \cdot 1 \frac{mV}{pC} \quad (6)$$

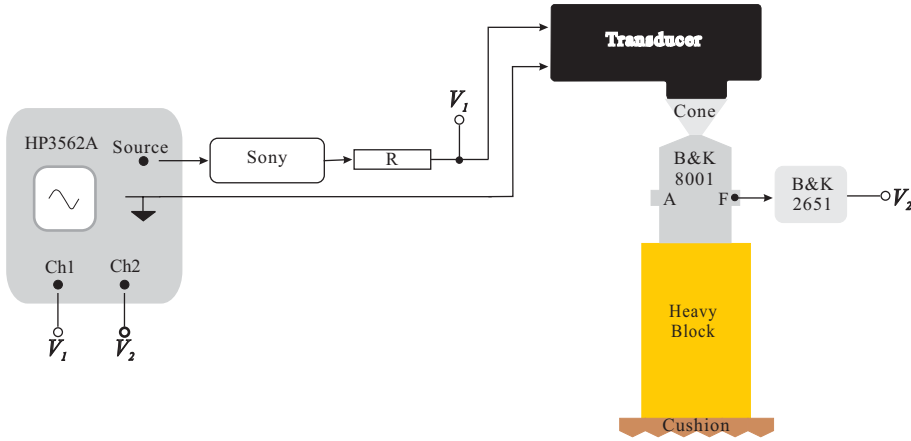


Figure 6: Measurement of the variable  $Z_{21}$ .

The third variable  $Z_{12}$  is the relation between the measured voltage  $V_1$  at the input terminals ( $i_1 = 0$ ) and the stimulation velocity  $v = i_2$  at the output terminal, see figure 3. This relation is presented in equation (7) and the measurement setup is illustrated in figure 7. The mini-shaker B&K 4810 was stimulated with a signal (random noise or/and a sinus sweep) and to achieve the magnitude of the velocity of the vibrations into the transducer, the acceleration  $A$  was measured with the B&K 8001 and then integrated which corresponds to a division by  $j\omega$ . However, the output from the accelerometer is a voltage  $V_A$  that has to be compensated by dividing it with a sensitivity factor  $\alpha_A$  to yield the desired acceleration. The measured frequency response was  $V_1/V_A$ .

$$Z_{12} = \frac{V_1}{i_2} = \frac{V_1}{v} = \frac{V_1}{A/j\omega} = \frac{V_1}{V_A/\alpha_A} \cdot j\omega = \frac{V_1}{V_A} \cdot \alpha_A \cdot j\omega \quad (7)$$

The total sensitivity,  $\alpha_A$ , was calculated to  $0.00382 \text{ Vs}^2/\text{m}$  according to equation (8).  $\alpha_A$  is the sensitivity of the accelerometer in the B&K 8001 and the charge amplifier B&K type 2635.

$$\alpha_A = 3.82 \frac{\text{pC}}{\text{m/s}^2} \cdot 0.001 \frac{\text{V}}{\text{pC}} = 0.00382 \frac{\text{V}}{\text{m/s}^2} \quad (8)$$

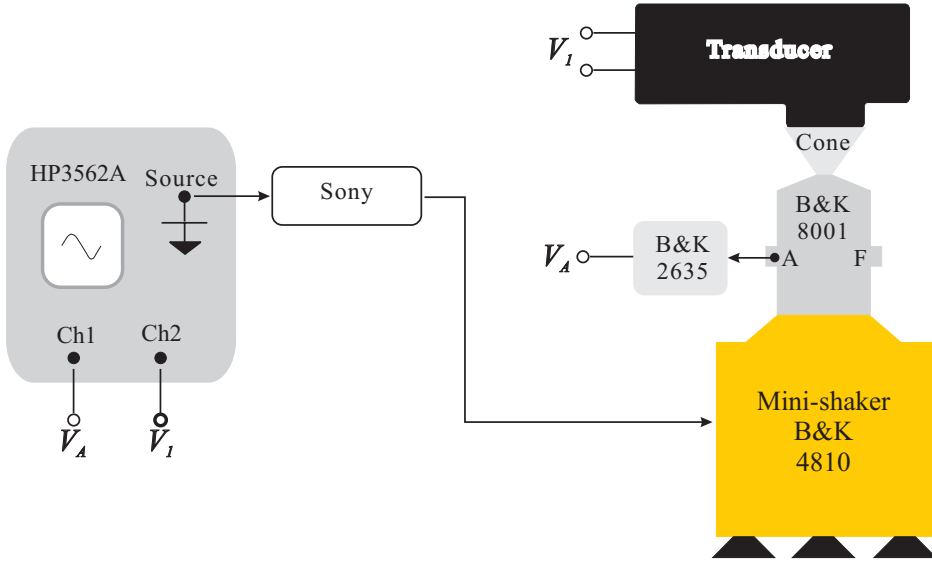
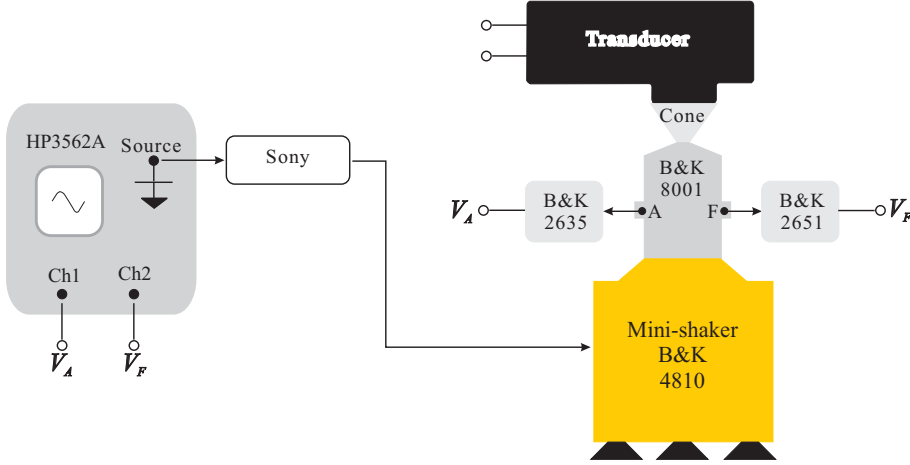


Figure 7: Measurement of the variable  $Z_{12}$ .

The last variable  $Z_{22}$  is as was mentioned before, the same as the mechanical output impedance of the transducer with  $i_1$  set to zero. The expression for this variable is given by equation (9). Figure 8 further shows the measurement setup. The true mechanical impedance is the difference between the measured impedance and the apparent mass  $m_{k0}$  measured during the calibration process. The measured frequency response was  $V_2/V_A$  and the sensibility factors  $\alpha_A$  and  $\alpha_F$  are the same as mentioned before.

$$Z_{22} = \frac{V_2}{i_2} = \left( \left[ \frac{F}{A} \right]_{\text{measured}} - m_{k0} \right) \cdot j\omega = \left( \frac{V_2}{V_A} \cdot \frac{\alpha_A}{\alpha_F} - m_{k0} \right) \cdot j\omega \quad (9)$$

Figure 8: Measurement of the variable  $Z_{22}$ .

### 2.3 The stimulation force

Considering the model equation (3) and figure 3, three equations: (10), (11) and (12) can be identified from which the stimulation force, i.e. the transfer function  $V_2/V_1$  can be derived.

$$V_1 = Z_{11} \cdot i_1 + Z_{12} \cdot i_2 \quad (10)$$

$$V_2 = Z_{21} \cdot i_1 + Z_{22} \cdot i_2 \quad (11)$$

$$V_2 = -i_2 \cdot Z_L \implies i_2 = -V_2/Z_L \quad (12)$$

Inserting (12) in (10) yields equation (13).

$$i_1 = \frac{\left( V_1 + \frac{Z_{12}}{Z_L} \cdot V_2 \right)}{Z_{11}} \quad (13)$$

If the equations (13) and (12) are put into equation (11) the result will be the searched relation as it is shown in the calculation steps (14), (15) and (16) yielding equation (17).

$$V_2 = \frac{Z_{21}}{Z_{11}} \cdot \left( V_1 + \frac{Z_{12}}{Z_L} \cdot V_2 \right) - \frac{Z_{22}}{Z_L} \cdot V_2 \quad (14)$$

$$\frac{Z_{21}}{Z_{11}} \cdot V_1 = V_2 \left( 1 - \frac{Z_{21}}{Z_{11}} \cdot \frac{Z_{12}}{Z_L} + \frac{Z_{22}}{Z_L} \right) \quad (15)$$

$$\frac{Z_{21}}{Z_{11}} \cdot V_1 = V_2 \left( \frac{Z_L Z_{11} - Z_{21} Z_{12} + Z_{22} Z_{11}}{Z_L Z_{11}} \right) \quad (16)$$

$$\frac{V_2}{V_1} = \frac{Z_L Z_{21}}{Z_L Z_{11} - Z_{21} Z_{12} + Z_{22} Z_{11}} \quad (17)$$

Equation (17) with units N/V shows the relation between the force output from the transducer over the voltage applied to it. This transfer function can simply be called the stimulation voltage to output force sensitivity of the transducer. Equation (17) was calculated and plotted in Matlab.

## 3 Results

Only the results from the swept sinus measurements are presented here due to the similarity with the results obtained with the noise random signal.

### 3.1 Mechanical impedance

The magnitude and the phase of the mechanical impedance of the skull of all the test persons are presented in figure 9. The frequency axis is logarithmic and the data covers the frequency range of 0.1 to 10 kHz. The mechanical impedance of the artificial mastoid 4930 from B&K is presented in each figure for comparison purpose.

Figure 10 indicates how the mechanical impedance of the skull changes with different static forces.

### 3.2 Two-port frequency response functions

In this section the magnitudes and the phases of the variables with the transducers B71 and BEST are presented. The frequency range of the data is the same as for the mechanical impedance data, 0.1 to 10 kHz. The transducer B71 nr. 86-5 is denoted as B71 and the BEST nr. 3 is denoted with the name B3.

The results for  $Z_{11}$  appear in figure 11,  $Z_{21}$  are shown in figure 12,  $Z_{12}$  are illustrated in figure 13 and for the last variable  $Z_{22}$  in figure 14.

### 3.3 The stimulation force

The results from the calculation of the frequency response from equation (17), i.e. the Stimulation Force (SF) are shown in the figures 15 to 18. The mechanical impedances of the test persons as well as the mechanical impedance of the Artificial Mastoid 4930 from B&K is used in the calculations instead of the load impedance  $Z_L$  in figure 4. In figure 15(a) the magnitude of the SF and its mean value are illustrated using the mechanical impedances of the thirty tested subjects and the four pole model variables measured with the transducer BEST nr. 3. Figure 15(b) shows the same quantities with the transducer B71. The mean value and standard deviation of the stimulation force for both transducers are presented in figure 16 (a) and (b).

The SF calculated with the mechanical impedance of the artificial mastoid instead of the tested subjects and with BEST is presented on figure 17(a). In the same figure, the mean value of the SF presented in figure 15(a) is

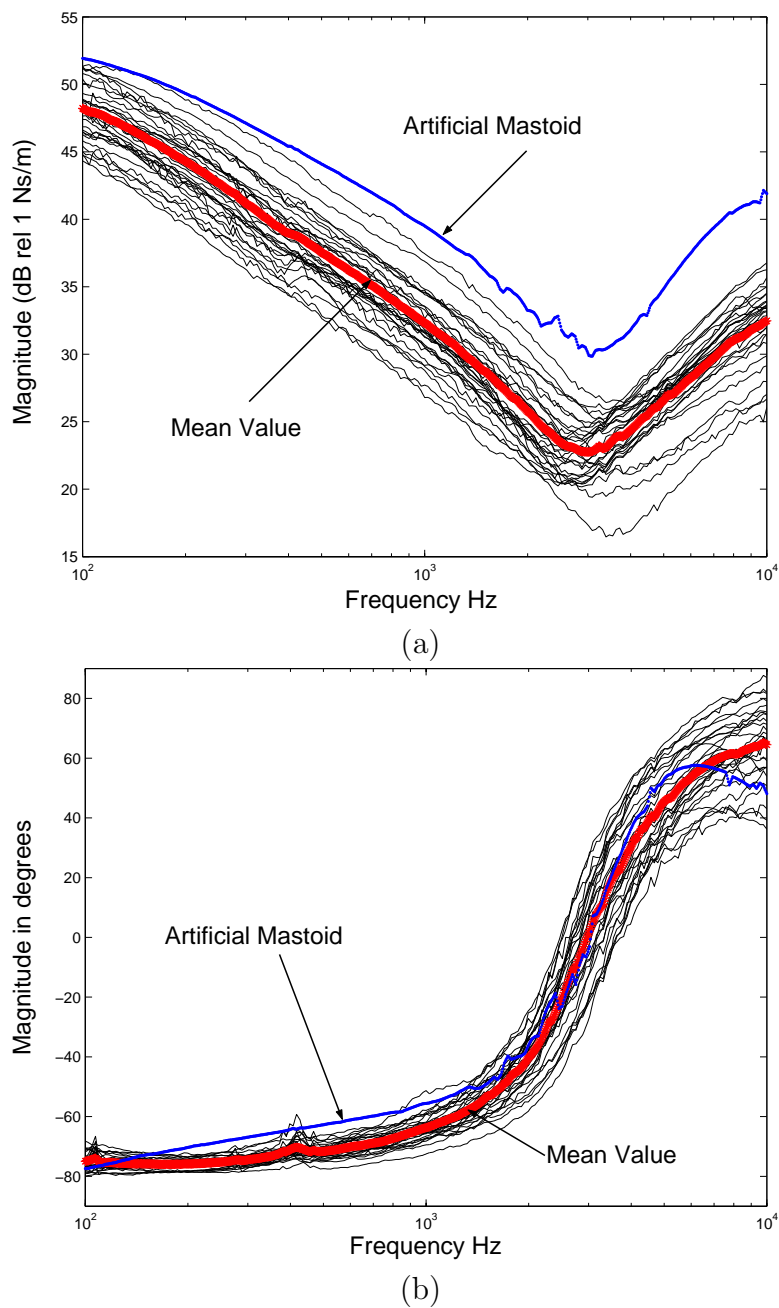
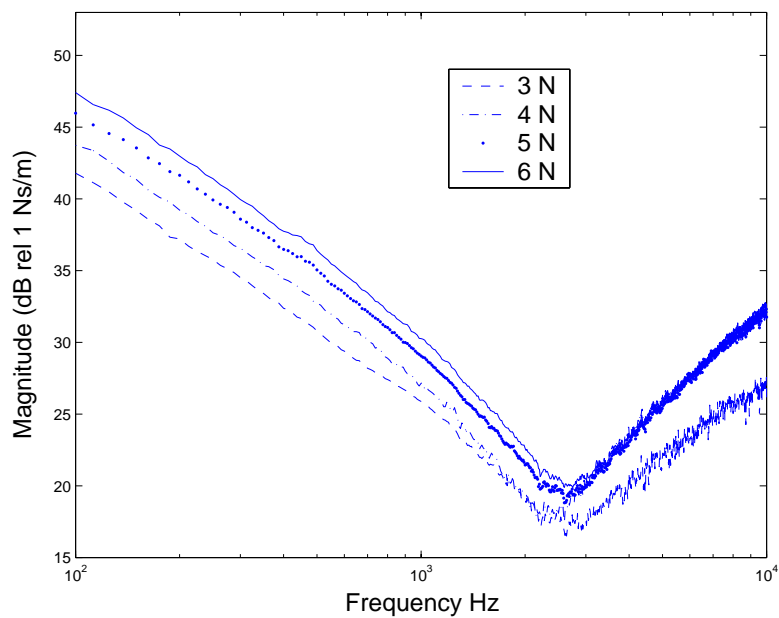
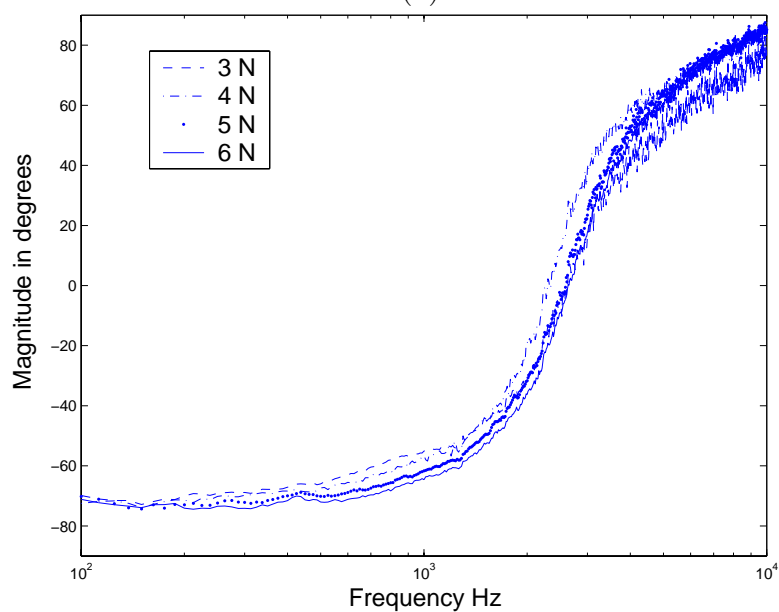


Figure 9: (a) Magnitude of the mechanical impedance of all 30 test subjects, mean value of the curves and magnitude of mechanical impedance of the artificial mastoid. (b) Phase of the same quantities.



(a)



(b)

Figure 10: (a) Magnitude and (b) phase of mechanical impedance of the skull of a test object, measured with different static forces.

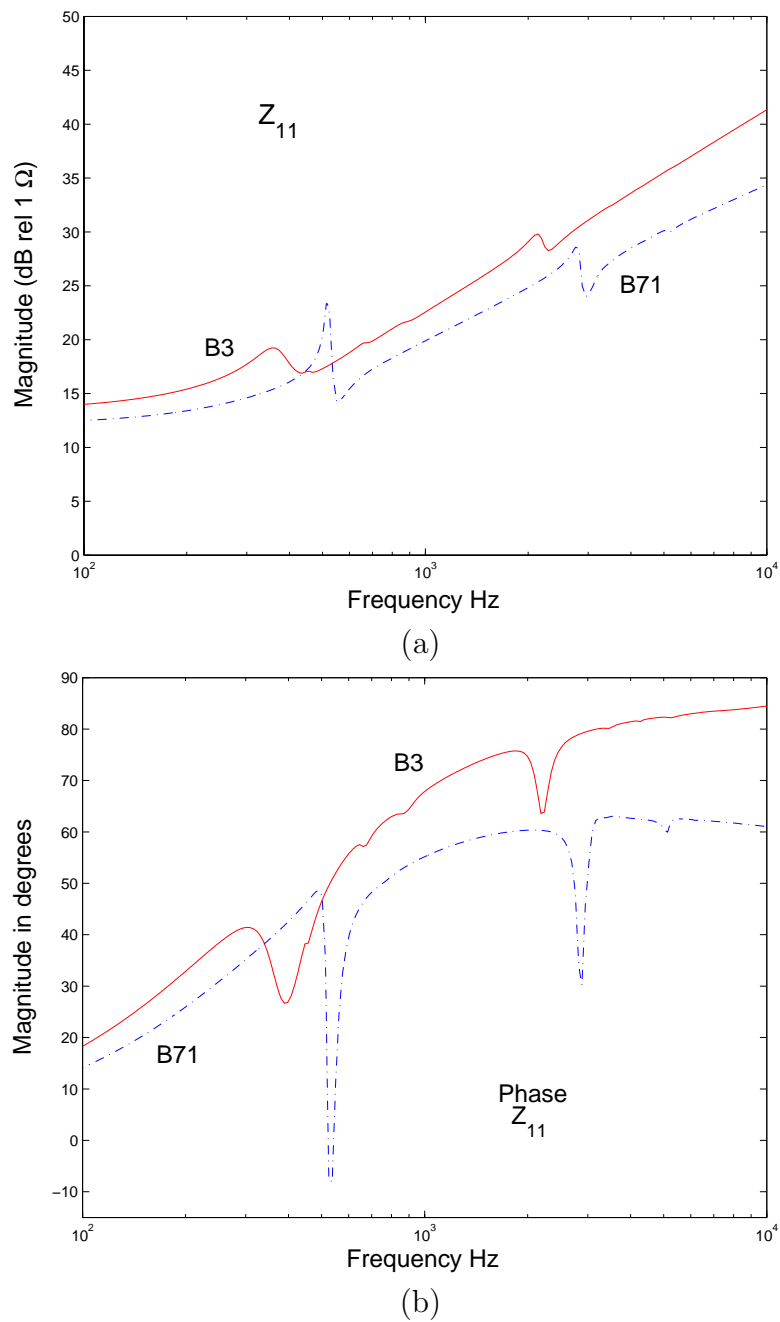


Figure 11: (a) Magnitude of the variable  $Z_{11}$  with BEST (B3) and B71, respectively. (b) Phase of  $Z_{11}$  with BEST (B3) and B71, respectively.

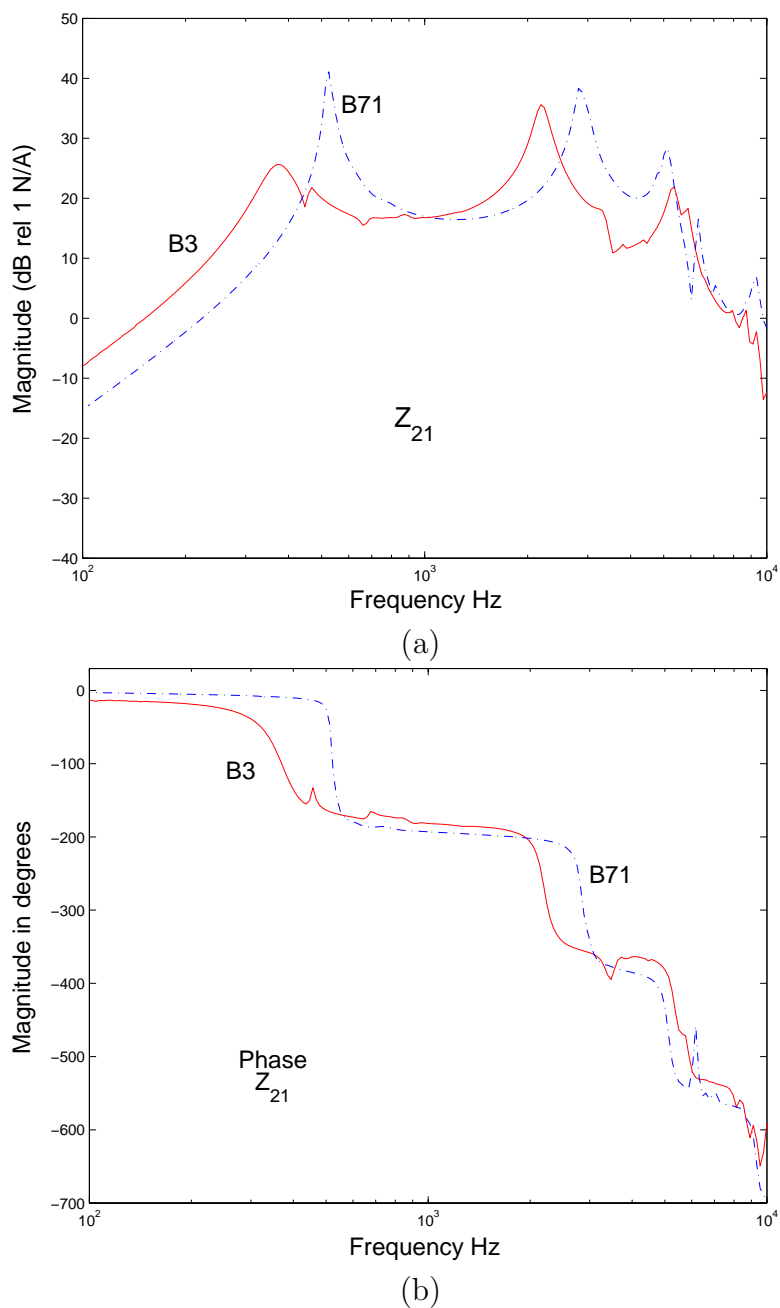
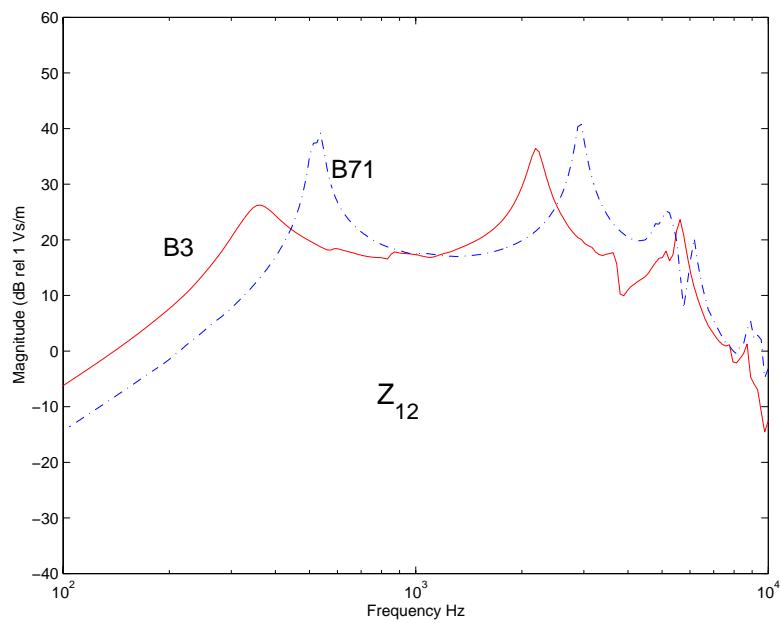
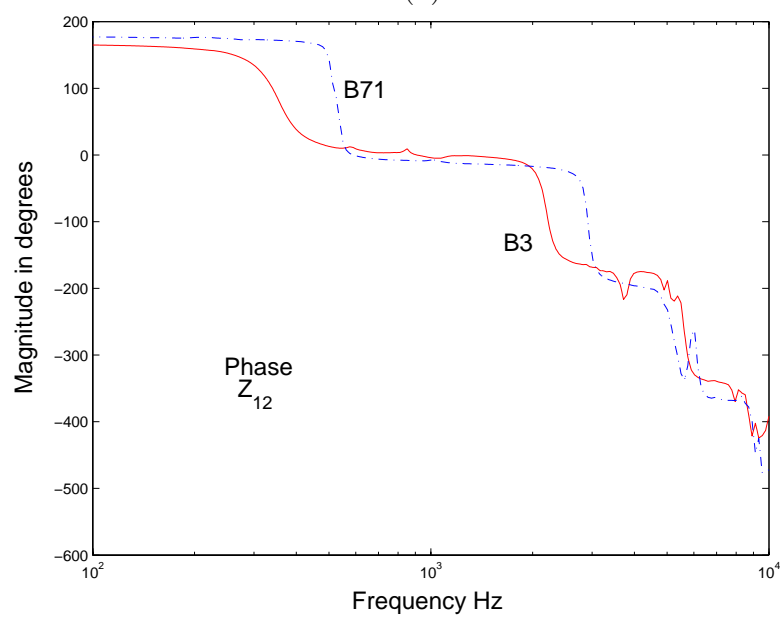


Figure 12: (a) Magnitude of the variable  $Z_{21}$  with BEST (B3) and B71, respectively. (b) Phase of  $Z_{21}$  with BEST (B3) and B71, respectively.

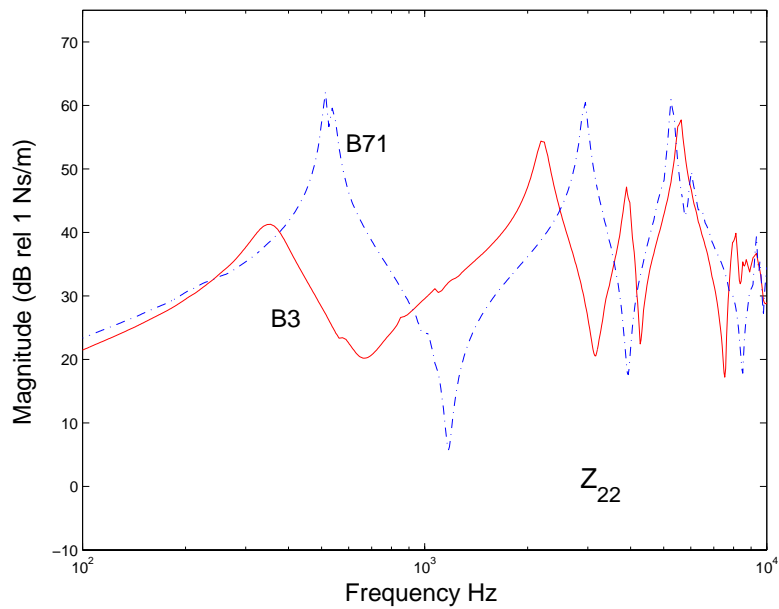


(a)

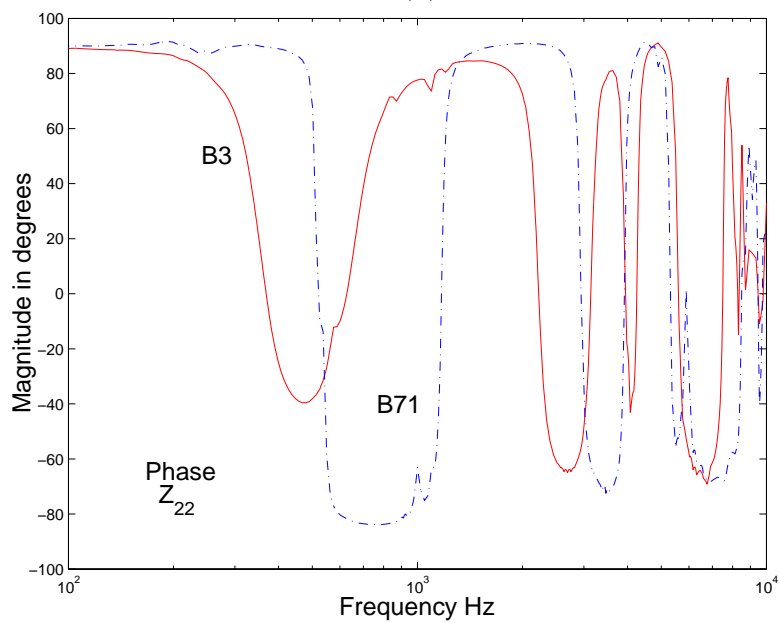


(b)

Figure 13: (a) Magnitude of the variable  $Z_{12}$  with BEST (B3) and B71, respectively. (b) Phase of  $Z_{12}$  with BEST (B3) and B71, respectively.



(a)



(b)

Figure 14: (a) Magnitude of the variable  $Z_{22}$  with BEST (B3) and B71, respectively. (b) Phase of  $Z_{22}$  with BEST (B3) and B71, respectively.

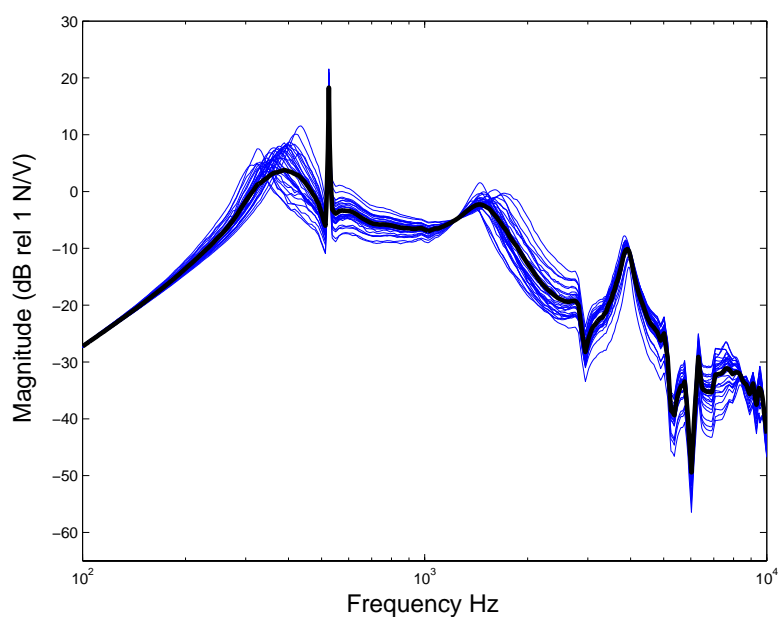
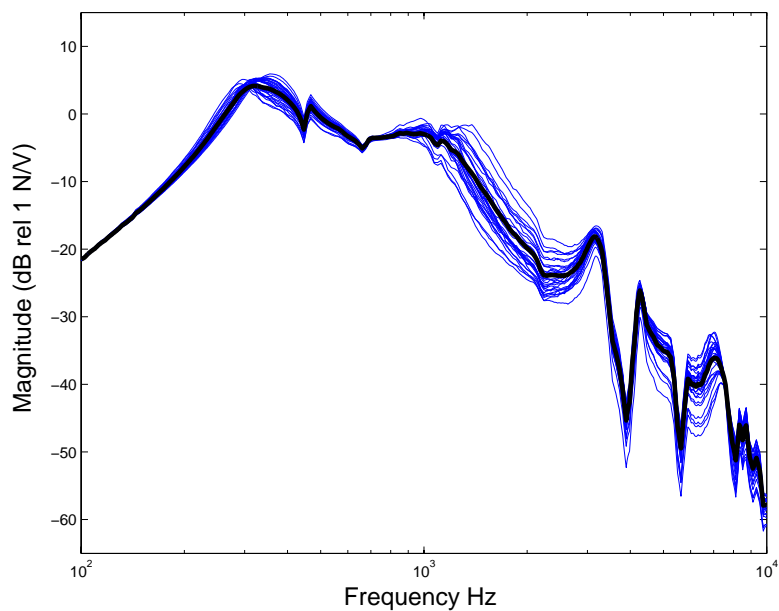


Figure 15: Magnitude of the stimulation force (SF) and its mean value, produced by the transducer BEST in (a) and by B71 in (b). The mechanical impedance of the skull of the thirty test subjects was used for this calculation.

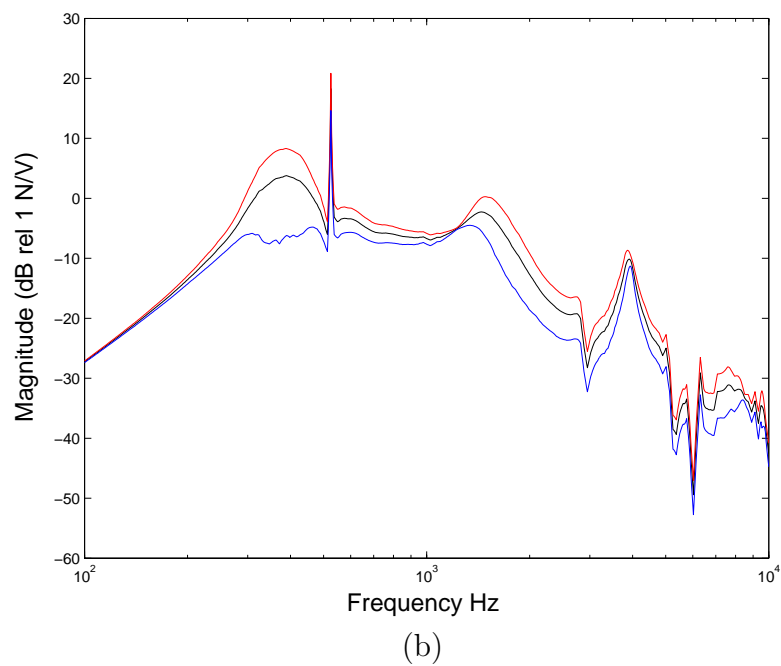
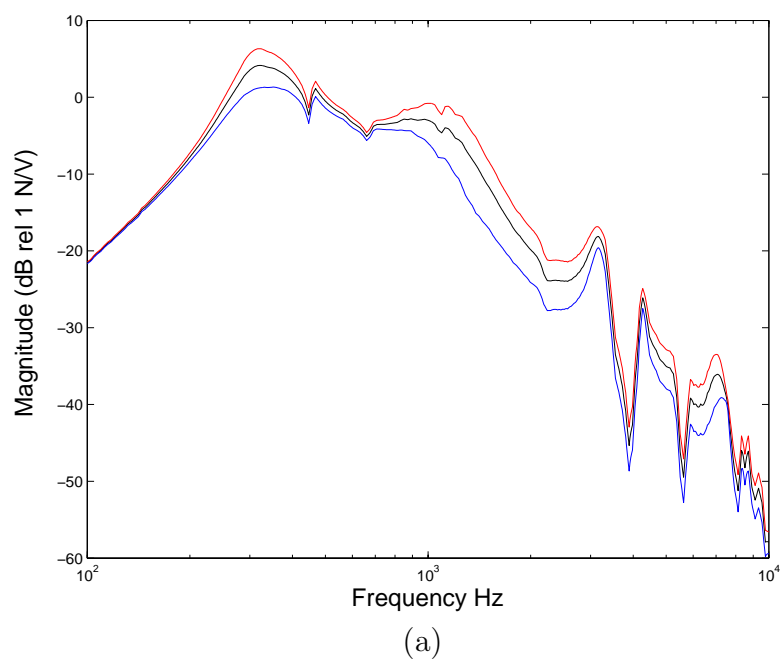
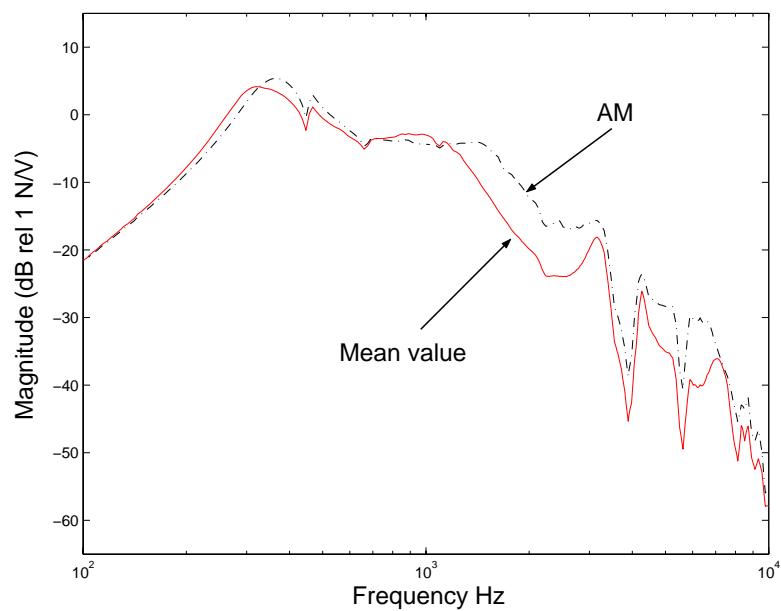


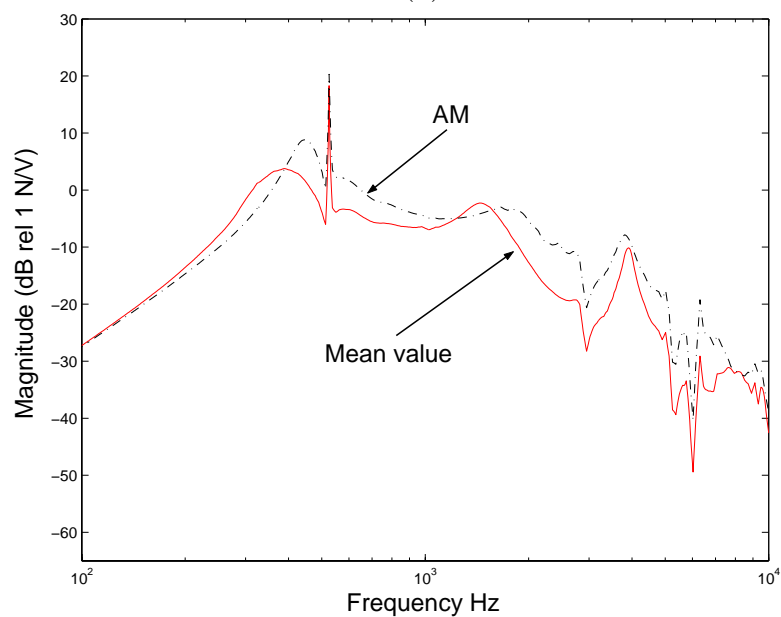
Figure 16: Mean value of the stimulation force (SF) and its standard deviation, produced by the transducer BEST in (a) and by B71 in (b). The mechanical impedance of the skull of the thirty test subjects was used for this calculation.

included. Figure 17(b) shows the corresponding result with the transducer B71. The mean value graph is the same as in figure 15(b).

Another comparison can be made between the stimulation forces calculated with the mean value of the mechanical impedance of the test persons as in figure 18(a) and the calculated with the mechanical impedance of the artificial mastoid (AM) as in figure 18(b). In both cases the force is calculated in the one hand with the model parameters measured with BEST and in the other hand with the parameters measured with B71.

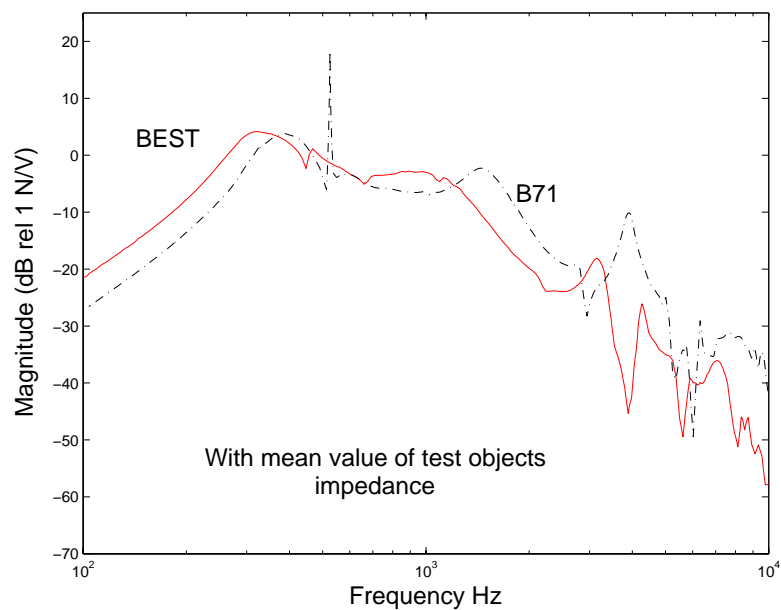


(a)

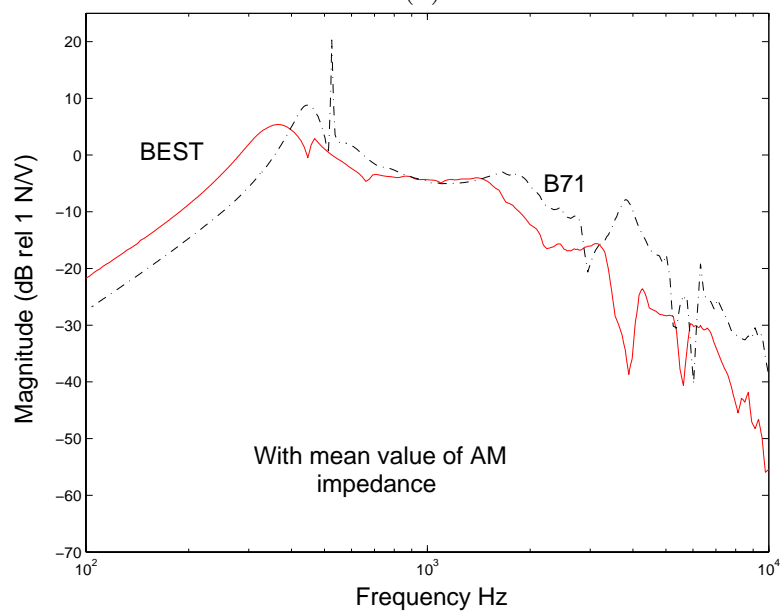


(b)

Figure 17: Comparison of the mean value of SF calculated with the mechanical impedance of the test subjects and the SF calculated with the mechanical impedance of the Artificial Mastoid (AM). The variables used were those measured with the transducer BEST (a) and B71 (b).



(a)



(b)

Figure 18: (a) The SF calculated with the mean value of mechanical impedance of the test persons and the model parameters measured with BEST and B71, respectively. (b) The same force calculated with the mechanical impedance of the AM and the model parameters measured with BEST and B71, respectively.

## 4 Discussion

### Mechanical impedance

To describe structural dynamic properties of the human skull by using a frequency response function, it is essential to assume that the system is linear. Investigators as Corliss and Koidan (1955), Smith and Suggs (1976), Flottorp and Solberg (1976), Khalil et al. (1979), Håkansson et al. (1986) and Håkansson et al. (1996) have stated that vibration transmission through the skull is linear at normal hearing levels, i.e. ordinary speech, and for frequencies ranging between 0.1 to 10 kHz.

In this investigation, no evident signs of nonlinear behavior was seen. The coherence values increased with increased signal levels, where the highest signal level was the speech level. The magnitude and phase response, at the same time, remained mainly unaffected. The mechanical impedance was measured at the skin surface over the temporal bone on the right side of the test persons and the measurements were made from 0.1 to 10 kHz. As Håkansson et al. (1986) found, the slope of the magnitude curves is negative and so is the phase up to 3000 Hz, which means that the impedance is stiffness controlled until it reaches the resonance frequency in the region of 3000 Hz. Above 3000 Hz the mechanical point impedance is mainly mass dominated. At the frequency of 3000 Hz the mass and the compliance cause a series resonance. The impedance varies for different persons and for all the test subjects, it appears to be generally lower than the impedance of the artificial mastoid (AM). The difference between the mean value of the subjects impedance and the impedance of the AM is generally about 4 to 10 dB. There is about 7 dB difference around the resonance frequency of 3000 Hz.

Measurements with different static forces were made, and it was observed that the impedance value became higher when the static force was increased reaching a steady state at around 6 N. Thus, the fact that the bone conduction hearing thresholds improve as the static force is increased and that the thresholds do not improve, reaching a steady state, for a static force greater than about 4-6 N is confirmed. According to the findings of Corliss and Koidan (1955), it is important that the static force is greater than 4 N but it seems unimportant whether the static force is 8 or 12 N.

### The frequency response functions or variables

Using the model in figure 3 it is possible to measure the variables and calculate the transfer function in equation (17). The behavior of  $Z_{11}$  is in accor-

dance with earlier measurements of electrical input impedance, Håkansson (2002), where at low frequencies the impedances of both transducers are resistive and mostly determined by the ohmic losses in the coil wires inside the transducers. BEST shows one first peak resonance, i.e. a parallel resonance, at 350 Hz that reflects the influence of the equivalent impedance  $Z_{eq}$  inside the transducer (fig. 4) which couples the electrical part of the transducer with the mechanical part. The first peak resonance for B71 appears at 513 Hz. A second, smaller peak resonance of both transducers appears around 1 to 2 kHz also here at different frequencies for both transducers. The influence of the equivalent impedance  $Z_{eq}$  is smaller since the value of  $Z_M$  increases at higher frequencies which implies smaller current  $v$ . At higher frequencies the electrical input impedances become inductive with a great difference in phase as seen in fig. 11(b), at the end of the frequency region. It indicates that the magnetic losses for B71 are greater than for BEST. BEST shows mostly inductive behavior reaching a phase near to 90 degrees, while B71 has a phase of 60 degrees. As earlier results have showed, Håkansson (2002), the magnitude of the parameter is 5 dB greater for BEST than for B71 over the whole frequency region.

Figures 12(a) and 13(a) show two main anti-resonances caused by the compliances and the masses in parallel in the mechanical part of the transducers. The first resonance is found at approximately 500 Hz and the second at approximately 2 kHz. At higher frequencies the housing of the transducers starts resonating in several modes causing resonances at the end of the frequency region. Unfortunately the variables do not present the peaks at exactly the same frequency which results in several artifacts when the calculation of the transfer function  $V_2/V_1$  is made. The reason of the displacement may be the assumption of no velocity in the measurement of  $Z_{21}$ , since the heavy block in figure 5 can be not enough heavy resulting in  $i_2 \neq 0$ . The difference in magnitude for both parameters is at least 10 dB at low frequencies until the first peak and at last 15 dB.

Variable  $Z_{22}$ , that is the mechanical output impedance of the transducers, is mass dominated at low frequencies causing one first anti-resonance (a maximum in impedance) at approximately 350 Hz for BEST and 500 Hz for B71. What follows is a series resonance at 700 Hz for BEST and 1.2 kHz for B71. A second anti-resonance appears due to the mass of the transducer's bobbin, coil, poles, vibrator plate and 1/3 of the housing and the compliance of the housing, at 2.2 kHz for BEST and 3 kHz for B71. A third anti-resonance at 4 and 5 kHz for BEST and B71, respectively, is caused by the mass of 2/3 of the housing and its compliance. BEST has 20 dB lower magnitude at the first anti-resonance frequency.

Figures 11(a), 12(a), 13(a) and 14(a) show that the damping of the spring

elements in BEST is better than in B71 since the resonance peaks are not so sharp. The resonances occur at a much lower frequency than for B71 which is due to the balanced construction of the suspension.

## Stimulation Force

It is important to compare the force calculated with the mechanical impedance of the test objects with that calculated with the mechanical impedance of the artificial mastoid, since the calibration of the measurement apparatus and hearing aids, at the audiology department at Sahlgren Hospital in Göteborg, is performed in accordance with the characteristics of the artificial mastoid. Specially since the results of the measurement of mechanical impedance show a mean difference of 7 dB between the test objects impedance and the impedance of the artificial mastoid.

The force for BEST does not differ so much from the force calculated with the AM's mechanical impedance, see fig. 17(a), except for the frequency region of 1.3 to 10 kHz where the difference can reach 10 dB. The B71 however, shows a similar difference between the force calculated with the same type of impedances but much earlier than BEST, from 400 Hz and along the remaining frequency range as seen in figure 17(b). Further, when comparing the force calculated with each transducer and each mechanical impedance (fig.18) it is observed that BEST gives some 5 dB higher amplitude from 100 to 400 Hz, in both cases of impedance, than B71. In the remaining frequency range, the magnitude of the force for B71 is higher (8 dB) between 1.2 to 3 kHz (mechanical impedance of test objects) and 1.5 to 3 kHz (mechanical impedance of AM).

A number of resonances appear along the frequency range which may depend on the fact that the parameters  $Z_{21}$  and  $Z_{12}$  do not have their resonance frequencies at the same place, they are displaced in relation with each other which might depend on the heavy block used for the measurement, since it was not an infinitely heavy mass. The force calculated with the parameters of BEST shows less spread than the force calculated with the parameters of B71 which is in accordance with the expected results.

Further comparisons can be performed if the component values of the transducers are computed from the parameter curves obtained in this work in order to do the same calculation of the force to observe if the appearing resonances are vanished or by measuring the frequency response  $V_{out}/V_{in}$  that Håkansson (2002) performed with the artificial mastoid and the HP-3562A.

## 5 Conclusions

Measurements of mechanical skin impedance of the human skull and mechanical impedance of the artificial mastoid (AM) from Brüel & Kjær has been performed. A four pole equivalent model of a bone conduction transducer with four variables that could be measured, was also made. Two transducers were used to measure the variables of the model in order to compare how the calculated output force of the transducers varies with load condition, where the load was the mechanical impedances of the test objects and the AM. The results obtained show what follows:

- The mechanical impedance of the human skull is lower than the mechanical impedance of the artificial mastoid from Brüel & Kjær with a mean difference of about 7 dB.
- The frequency response measurement shows lower amplitude for BEST than for B71 with an amount of 5 to 20 dB dependent of the measured variable, which depends on better damping of the spring elements in BEST.
- The resonance frequencies for BEST occur at a lower frequency than for B71 due the balanced construction of BEST.
- Though the great difference for the two mechanical impedances (human skull and AM), the output force calculated with the impedances does not differ so much for BEST as for B71, where the difference is more evident from 400 Hz and upwards. For BEST the main difference is of approximately 8 dB in the frequency range of 1 to 3 kHz. See fig. 17.
- In the comparison of the output force obtained with each transducer and the same load impedance, shown in fig.18 it is observed that BEST has 5 dB higher amplitude in the low frequency region between 100 and 400 Hz. In the high frequency region beginning at 1.3 to 1.5 kHz however, B71 has a higher amplitude of about 8 dB.

## 6 Acknowledgment

I have to thank my supervisor Bo Håkansson for all the time he was sitting, discussing and explaining different things I did not see as easily as he does. He has been an inspiration for me during this work.

I would also like to thank all the voluntaries for helping me during the measurements of mechanical impedance. Further, I want to thank Fredrik Athley, Christopher Brown, Jesper Bank and Karin Althoff at the department of Signals and Systems because they introduce me to the world of L<sup>A</sup>T<sub>E</sub>X and patiently helped me when I got frustrated.

Finally, I want to thank Andreas and my children for all support they always give to me.

This investigation was financially supported by a grant from Stingerfonden.

## References

- Bendat, J. and Piersol, A. (1980). *Engineering Applications of Correlations and Spectral Analysis*. McGraw-Hill, New York.
- Corliss, E. L. R. and Koidan, W. (1955). “Mechanical impedance of the forehead and mastoid”. *J. Acoust. soc. Am.*, 27(6):1164–1172.
- Flottorp, G. and Solberg, S. (1976). “Mechanical impedance of human head-bones (forehead and mastoid portion of temporal bone) measured under ISO/IEC conditions”. *J. Acoust. soc. Am.*, 59(4):899–906.
- Håkansson, B., Carlsson, P., Brandt, A., and Stenfelt, S. (1996). “Linearity of sound transmission through the human skull *in vivo*”. *J. Acoust. Am.*, 99(4):2239–2243.
- Håkansson, B., Carlsson, P., and Tjellström, A. (1986). “The mechanical point impedance of the human head, with and without skin penetration”. *J. Acoust. Am.*, 80(4):1065–1075.
- Håkansson, B. E. V. (2002). “The Balanced Electromagnetic Separation Transducer: A new bone conduction transducer”. *Submitted to J. Acoust. Soc. Am.*
- Khalil, T., Viano, D., and Smith, D. L. (1979). “Experimental analysis of the vibrational characteristics of the human skull”. *J. Sound Vib.*, 63(3):351–376.
- Smith, J. B. and Suggs, C. W. (1976). “Dynamic properties of the human head”. *J. Sound Vib.*, 48(1):35–43.